Journal of Chromatography A, 1217 (2010) 530–539

Contents lists available at ScienceDirect

Journal of Chromatography A

journal homepage: www.elsevier.com/locate/chroma

Surfactant-bound monolithic columns for separation of proteins in capillary high performance liquid chromatography

Congying Gu [a], Jun He [a], Jinping Jia [b], Nenghu Fang [c], Robert Simmons [a], Shahab A. Shamsi [a,*]

[a] Department of Chemistry, Center for Biotechnology and Drug Design, Georgia State University, 38 Peachtree Center Ave, Atlanta, GA 30303, USA
[b] Department of Environmental Science and Engineering, Shanghai Jiao Tong University, Shanghai, 200240, China
[c] Department of Chemistry and Chemical Engineering, Shanghai Jiao Tong University, Shanghai, 200240, China

ARTICLE INFO

Article history:
Received 11 November 2009
Accepted 25 November 2009
Available online 3 December 2009

Keywords:
11-Acrylaminoundecanoic acid (AAUA)
D-optimal design
Monolithic column
Physical and chromatographic properties
Protein and protein digest separation

ABSTRACT

A surfactant-bound monolithic stationary phase based on the co-polymerization of 11-acrylaminoundecanoic acid (AAUA) is designed for capillary high performance liquid chromatography (HPLC). Using D-optimal design, the effect of the polymerization mixture (concentrations of monomer, crosslinker and porogens) on the chromatographic performance (resolution and analysis time) of the AAUA–EDMA monolithic column was evaluated. The polymerization mixture was optimized using three proteins as model test solutes. The D-optimal design indicates a strong dependence of chromatographic parameters on the concentration of porogens (1,4-butanediol and water) in the polymerization mixture. Optimized solutions for fast separation and high resolution separation, respectively, were obtained using the proposed multivariate optimization. Differences less than 6.8% between the predicted and the experimental values in terms of resolution and retention time indeed confirmed that the proposed approach is practical. Using the optimized column, fast separation of proteins could be obtained in 2.5 min, and a tryptic digest of myoglobin was successfully separated on the high resolution column. The physical properties (*i.e.*, morphology, porosity and permeability) of the optimized monolithic column were thoroughly investigated. It appears that this surfactant-bound monolith may have a great potential as a new generation of capillary HPLC stationary phase.

1. Introduction

The advantages of capillary high performance liquid chromatography (HPLC) over conventional normal scale HPLC have long been recognized. The advantages include increased chromatographic resolution, higher efficiency, lower sample consumption, the ability to analyze and isolate rare compounds of interest, reduced solvent consumption, greater mass sensitivity [1–4] and convenient on-line connection to mass spectrometer [5–7].

Polymeric monolithic stationary phases offer alternatives to the classical microparticulate sorbents and provide certain advantages for sample analysis. In contrast to the traditional stationary phases, which consist of packed particles, the monolithic separation medium is made of a continuous, rigid polymeric rod with a porous structure. The lack of intraparticular void volume improves mass transfer and separation efficiency, allowing fast, high-quality separations. Due to these unique properties, monolithic material has attracted notable attention and great improvements have been achieved in this field [8–10]. A large number of new and attractive application have been introduced in broad fields such as biological [11–15], environmental [16–18] and pharmaceutical [19–22] analysis. The ever increasing popularity of monolithic stationary phases stimulates the thorough studies into the preparation mechanism as well as exploration of new kind of monolith.

For polymer monolithic column, the column performance significantly depends on the pore structure of the monolithic material, which is finally controlled by the composition of the polymerization mixture [10,23–25]. Therefore, to explore a new monolith with appropriate properties for certain use, the research work should optimize the composition of the polymerization mixture.

Traditionally, optimization is often done by varying one-factor-at-a-time while keeping the others constant. This univariate approach could be used to study the effect of one factor to the responses but fails when interaction of more than one factor is involved. Experimental design is a multivariate method, which allows one to obtain appropriate response that can be analyzed to study the individual effects and the interaction effects of several factors. Thus, the method can be effectively utilized to determine the optimum conditions through a relatively smaller number of experiments. Currently, the multivariate method has been more and more widely used in optimization studies [26–31].

* Corresponding author. Tel.: +1 404 413 5512; fax: +1 404 413 5551.
E-mail address: chesas@langate.gsu.edu (S.A. Shamsi).

0021-9673/$ – see front matter © 2009 Elsevier B.V. All rights reserved.
doi:10.1016/j.chroma.2009.11.082

In recent years, development of polymer-based monolithic columns has attracted considerable attention as significant alternative stationary phases for separation of macromolecules such as proteins and polypeptides in capillary HPLC [15,32–34]. In this study, we use three proteins (ribonuclease A, cytochrome *c* and myoglobin) as the model test analytes to evaluate the chromatographic properties of a novel methacrylate derived surfactant-bound monolithic column. We initially tried using vinyl terminated surfactants (synthesized previously by our research group), which are well documented as very useful pseudostationary phases for MEKC [35–39]. Although vinyl terminated surfactant monomers form stable micelles in aqueous solution, they do not form stable monoliths when crosslinked with EDMA. This failure motivated us to synthesize methacrylated surfactant monomer with a conjugated double bond at the end of the hydrophobic tail and a polar carboxyl head group that has the potential to provide hydrogen bonding and electrostatic interactions. A multivariate, D-optimal design is introduced to optimize the preparation of this new kind of monolithic column. The essential parameters in column preparation, which influence the chromatographic performance of the monolith, were systemically evaluated and optimized.

2. Experimental

2.1. Chemicals and standards

The reagents ethylene glycol dimethacrylate (EDMA), 1-propanol, 2,2′-azobisisobutyronitrile (AIBN), 11-aminoundecanoic acid were from Aldrich (Milwaukee, WI, USA); γ-methacryloxypropyl-trimethoxysilane, acryloyl chloride and ribonuclease A, cytochrome c, myoglobin and trypsin were purchased from Sigma (St. Louis, MO, USA). 1,4-Butanediol, butyl methacrylate were purchased from Fluka (Buchs, Switzerland). All the reagents were used as received except for the EDMA, which was purified by distillation under vacuum prior to use.

2.2. Preparation of 11-aminoundecanoic acid (AAUA)

The AAUA monomer was prepared according to procedure reported by Yeoh et al. [40]. First, an aqueous solution of ethanol (250 mL ethanol/35 mL distilled water) was used to dissolve 10 g (0.05 mol) of 11-aminoundecanoic acid. To this solution, 6 g (0.15 mol) of NaOH was added slowly until a clear solution is obtained. Next, 6 mL (0.072 mol) of acryloyl chloride was added dropwise and the reaction mixture stirred for approximately three hours at just below 10 °C, after which it was filtered. The filtrate was acidified with diluted hydrochloric acid and washed with triply deionized water. The white precipitate formed was collected after filtration. The crude product was recrystallized from aqueous ethanol, filtered and dried by lyophilization. The yield of the synthesis is around 70%. The critical micellar concentration of sodium salt form of AAUA is 5×10^{-3} mol/L at 25 °C. The purity of AAUA was checked by electrospray ionization mass spectrometry (ESI-MS), ^{1}H NMR and elemental analysis (data not shown).

2.3. Preparation of monolithic columns

For the preparation of stationary phases the inner walls of the capillaries were vinylized with 3-(trimethoxylsilyl)propyl methacrylate. The procedure can be found elsewhere [41,42]. Subsequently, AAUA, EDMA, 1-propanol, 1,4-butanediol, water, and AIBN were mixed ultrasonically into a homogenous solution and purged with nitrogen for 10 min. A 45 cm long vinylized capillary was filled with the polymerization mixture up to a length of 35 cm, sealed with rubber septum, and then placed in a GC oven to polymerize for 20 h at 60 °C. The ternary porogenic system including 1,4-butanediol, 1-propanol and water was borrowed from Peters et al. work [43]. Every column required by the experimental design was made in duplicate. After the polymerization was completed, the monolithic column was washed with methanol for 12 h using a HPLC pump to remove unreacted monomers and porogens. An on-column detection window was made next to the polymer bed using a thermal wire stripper. Finally, the column was cut to 45 cm with an effective length of 30 cm.

2.4. Morphology, pore size and surface area measurements

The microscopic morphology of the monoliths was evaluated using scanning electron microscope with the aid of a Hitachi X-650 (Hitachi, Japan) SEM apparatus at 7.5 kV and a filament current of 40 mA. Monolithic column samples were fractured, cut to a length of 2 mm, and placed on an aluminum stub by means of double sided carbon tape. Then they were sputter-coated with a gold/palladium alloy using a SPI Sputter (SPI Supplies Division of Structure Probe, West Chester, PA, USA) for 1 min at 30 mA to prevent charging.

Pore-size distributions data were obtained by AutoPore IV 9500 mercury intrusion porosimetry (MIP_y, Mcirometics Instrument Corporation, GA, USA). Surface area data were obtained by nitrogen adsorption measurements performed on Micromeritics TriStar 3000 (Micromeritics Instrument Corporation, GA, USA). The specimens for the measurement of pore-size distribution and surface area were prepared in parallel polymerization in glass vials under the same conditions with the same mixtures. Once the polymerization was completed, Soxhlet extraction of the monolith was carried out with methanol for 24 h. After drying the monoliths at 70 °C for 24 h under vacuum, nitrogen adsorption and mercury intrusion porosimetry experiments were performed.

2.5. Capillary HPLC instrumentation

The HPLC chromatographic experiments were carried out on an Ultra-Plus & Ultra-Plus II Micro LC system (Micro-Tech Scientific, Sunnyvale, CA, USA) equipped with a Data Module UV–visible detector (wavelength continuously adjustable) and *ChromPerfect*® (Version 5.1, Justice Laboratory Software, NJ, USA) software. A Series III HPLC pump (Lab Alliance, State College, PA, USA) was used for washing and equilibrating the monolithic column. Fused silica capillary (O.D. 375 μm, I.D. 100 μm) was obtained from PolymicroTechnologies Inc. (Phoenix, AZ, USA).

2.6. HPLC chromatographic conditions

Gradient elution was used for the protein separation in capillary HPLC. Mobile phase A: 98% ACN with 0.1% TFA in water; mobile phase B: 2% ACN with 0.1% TFA in water. Linear gradient program: 16% A at 0 min and 40% A at 0.5 min. The flow rate was 1.1 μL/min and the injection volume was 100 nL. UV detection was carried out at 214 nm.

2.7. Tryptic protein digest preparation

Ten milligrams of myoglobin was dissolved in 10 mL of 50 mM ammonium bicarbonate solution. To this solution 0.1 mg trypsin was added providing a substrate-to-enzyme ratio of 100:1, and then the solution was incubated in a water bath for 20 h at 37 °C. At last, the digest was vacuum-dried and reconstituted in water without any additional cleanup steps before analysis [44].

2.8. Calculations

The resolution (*Rs*) was calculated by the *ChromPerfect*® software.

Table 1
D-optimal design and the level of factors used for the optimization of protein separation in μ-HPLC.

Variable factors[a]	Levels	
	Lower limit (−1)	Upper limit (+1)
A: % (w/w) EDMA	18.5	21.3
B: % (w/w) AAUA	1.8	7.0
C: % (w/w) 1-propanol	60.0	74.0
D: % (w/w) 1,4-butanediol	0	12.0
E: % (w/w) water	2.0	12.0

[a] Restriction: $A+B+C+D+E=99.5\%$ (w/w), 0.5% (w/w) fixed AIBN.

The porosity of the monolith prepared in capillary was examined by a flow method [1]. Briefly, the mobile phase linear velocity was measured by an inert tracer (thiourea) and the volumetric flow rate was also measured. Then with the known empty tube dimension, the total porosity ε_T was calculated using the following Eq. (1):

$$\varepsilon_T = \frac{V}{\pi r^2 u} \times 100\% \quad (1)$$

where V (m^3/min) is the volumetric flow rate of mobile phase. r (m) is the inner radius of the empty column. u (m/s) is the linear velocity of mobile phase, which was determined by unretained compound thiourea. The average value of the porosities obtained at different flow rates was regarded as the total porosity of the monolith.

The permeability (K^0) of a porous medium is a measure of its capacity to transmit a fluid driven by an imposed pressure drop across the column. Darcy's law linking the solvent viscosity and column porosity to K^0, which was calculated as follows:

$$K^0 = \frac{u\eta L\varepsilon_T}{\Delta p} \quad (2)$$

where η (Pa s) is the dynamic viscosity of eluent. L (m) is the effective column length and Δp (Pa) is the pressure drop [45].

2.9. Experimental design

Design-Expert (version 7.0.3, Stat-Ease, Inc. Minneapolis, MN) was used to generate D-optimal experimental designs, data processing (statistical calculations), contour plots and optimum conditions. The D-optimal design variables include five factors: *A*, concentration of the crosslinker (% w/w EDMA); *B*, concentration of the monomer (% w/w AAUA); *C*, concentrations of 1-propanol (% w/w 1-propanol); *D*, concentration of 1,4-butanediol (% w/w 1,4-butanediol); and *E*, concentration of water (% w/w water) [24]. The constraints and the levels of the factors are listed in Table 1. Three proteins ribonuclease A, cytochrome *c* and myoglobin were used as model test analytes. Average resolution ($Rs_{(avg)}$) and analysis time (t_R, measured as the retention time of the last protein myoglobin) were used as the responses (Table 2). All the data obtained from the actual experiments were input into the Design-Expert software. After which the data were fitted into mixture quadratic model which was chosen based on the *F*-test and lack-of-fit test. The observed effects were tested for significance using analysis of variance (ANOVA). The 2D contour plots were created by the software to show the interactions between significant factors. Finally, the optimum combination was detected using Desirability function available in Design-Expert software.

3. Results and discussion

The synthesized AAUA monomer has a C_{11} long hydrocarbon chain, which is supposed to provide hydrophobic interactions. Note that the COOH group could provide hydrogen bond interactions between the analytes and stationary phase and could also be ionized depending upon the pH of the mobile phase. Additionally, the acrylamide group makes possible to use free radical polymerization to prepare monolith.

Table 2
Resolution and total run time data gathered from the D-optimal experimental design run order for multivariate optimization of surfactant based monolithic columns.

Column	Variable factors					Responses	
	EDMA (%, w/w)	AAUA (%, w/w)	1-Propanol (%, w/w)	1,4-Butanediol (%, w/w)	Water (%, w/w)	$Rs_{(avg)}$[a]	t_R[b] (min)
1	21.3	7.0	60.0	0	11.2	n.a.	n.a.
2	19.9	1.8	60.0	5.8	12.0	2.8	3.8
3	18.5	7.0	60.0	1.5	12.5	12.4	30
4	21.3	7.0	69.2	0	2.0	5.9	3.3
5	19.9	1.8	63.8	12	2.0	5.4	7.5
6	21.3	4.2	60.0	12	2.0	5.7	6.0
7	21.3	1.8	74.0	0.2	2.2	1.3	1.9
8	18.5	1.8	67.2	0	12	4.0	3.9
9	19.2	2.9	69.6	2.1	5.7	2.1	2.0
10	18.5	7.0	60.0	2.0	12.0	12.8	36
11	19.9	1.8	63.8	12	2.0	5.0	2.5
12	21.3	1.8	74.0	0.2	2.2	1.2	2.1
13	21.3	4.2	60.0	12	2.0	4.7	2.7
14	18.5	7.0	72.0	0	2.0	2.9	2.1
15	19.9	3.6	74.0	0	2.0	2.8	2.5
16	18.5	7.0	60.0	12	2.0	5.1	5.8
17	21.3	4.0	62.2	0	12.0	8.4	15
18	19.2	2.9	64.4	3.9	9.1	3.7	2.8
19	19.2	4.2	62.6	8.1	5.4	3.8	2.2
20	18.5	1.8	60.0	12	7.2	2.5	2.8
21	18.5	1.8	69.6	7.6	2.0	0.9	2.0
22	18.5	7.0	67.0	0	7.0	7.1	10
23	18.5	7.0	66.0	6.0	2.0	3.7	2.1
24	21.3	7.0	69.2	0	2.0	2.8	2.6
25	19.8	7.0	62.9	2.9	6.9	6.3	5.7

n.a.: Not available due to high back pressure exceeding the upper limit of 5000 psi of the HPLC pump.
[a] $Rs_{(avg)}$ is the average resolution of the three proteins.
[b] t_R is the retention time of the last peak (myoglobin).

3.1. Experimental design

3.1.1. Parameters for D-optimal experimental design

According to previous studies [10,25,46], varying the ratio of the components of the polymerization mixture generates monolithic columns with different properties (*e.g.*, physical properties and chemical properties), from which different retention performances are expected. The D-optimal design is very appropriate for cases where some of the factors can only be varied over a restricted area, hence, generating an irregular experimental domain in which orthogonality is not obtained [47]. In this study, composition of polymerization mixture is subjected to such restrictions, and based on this rationale a D-optimal design was used [48].

The % (w/w) AAUA, % (w/w) EDMA, % (w/w) 1-propanol, % (w/w) 1,4-butanediol and % (w/w) water within the polymerization mixture were set as variable factors in the experimental design. The constraints for all the factors summarized in Table 1 were set based on preliminary experiments. The % (w/w) EDMA in the polymerization mixture was set in the range of 18.5–21.3%. When % (w/w) EDMA was below 18.5%, the generated monolith was found to have poor mechanical stability. On the other hand, % (w/w) EDMA higher than 21.3% was not effective for the permeability of the monolith. The concentration ranges of the AAUA monomer was also determined by the preliminary studies. It was found that when the % (w/w) AAUA was higher than 7.0%, it results in an inhomogeneous polymerization mixture. Therefore, 7.0% (w/w) AAUA was set as the upper limit. When the % (w/w) AAUA was lower than 1.8%, the monolithic column demonstrated poor performance in capillary HPLC separation. The range of % (w/w) 1-propanol (60.0–74.0%) was set according to previous studies [46,49–51]. For 1,4-butanediol, higher than 12.0% (w/w) of 1,4-butanediol provided an inhomogeneous monolith matrix. Hence, the % (w/w) 1,4-butanediol was set from 0% to 12%. As for the water content, when the % (w/w) water lower than 2.0%, the monolith gives poor resolution in protein separation. However, higher than 12.0%, provides an inhomogenous polymerization mixture. Nevertheless, the total concentration of the five components was kept at 99.5% (w/w) and the initiator, AIBN, was fixed at 0.5% (w/w). A total of five design variables were studied at two levels, and this resulted in a final experimental matrix consisting 25 experiments.

Table 2 demonstrates the 25-run experimental plan and the responses. The chromatographic parameters such as average resolution ($Rs_{(avg)}$) and retention time (t_R) of the last peak were chosen as the responses of the experimental design study. The ranges of $Rs_{(avg)}$ were found to be from 0.9 to 12.8, whereas t_R ranged from 1.9 min to 36.0 min. Fig. 1(A and B) shows two of the representative chromatograms for the proteins obtained from the D-optimal design experiments (*e.g.*, experiment 10 and experiment 7, Table 2), respectively. The experiment 7 represents one of the fastest separations among all experiments. However, experiment 10 demonstrated one of the separations with highest resolution for the three proteins. This trend indicated that the composition of the polymerization mixture has a significant effect on the chromatographic performance of the yielded monolith and should be carefully optimized.

3.1.2. Validation of models

A mixture quadratic model was developed for each of the response parameters. The yielded model is a mathematical equation which is useful for identifying the relative significance of the factors by directly comparing the factor coefficients. For mixture quadratic model, the fitted equation is in the form of Eq. (3):

$$y = \beta_0+\beta_1A+\beta_2B+\beta_3C+\beta_4D+\beta_5E+\beta_{12}AB+\beta_{13}AC+\beta_{14}AD + \beta_{15}AE+\beta_{23}BC+\beta_{24}BD+\beta_{25}BE+\beta_{34}CD+\beta_{35}CE+\beta_{45}DE \quad (3)$$

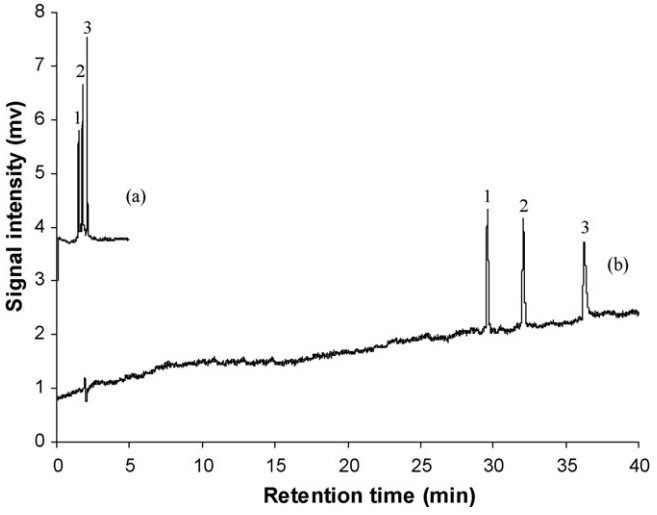

Fig. 1. The representative chromatograms for separation of proteins on (a) column 7 and (b) column 10. Conditions: mobile phase A: 98% ACN with 0.1% TFA in water; mobile phase B: 2% ACN with 0.1% TFA in water; linear gradient program, 16% A at 0 min, 40% A at 0.5 min; injection volume, 100 nL; flow rate, 1.1 μL/min; detection, 214 nm. Solutes: (1) ribonuclease A; (2) cytochrome *c*; (3) myoglobin. Each analytes was injected at concentration of 0.3 mg/mL in water.

where y is the predicted response. β_0 is the intercept. The first-order mixture-model coefficient β_n ($n = 1, 2, 3, 4, 5$) is the coefficient for the input factor (A, B, C, D and E) which predicts the response from the pure components. $\beta_{12}, \beta_{13}, \beta_{14}, \ldots$ is the coefficient for the two factors interaction (AB, AC, AD, ...), which describes the effect of their interaction on the response. Positive interaction coefficients indicate the corresponding factor is directly proportional to the response. On the other hand, the negative interaction coefficients means the factor is inversely proportional to the response.

The significance of the calculated empirical model was assessed by ANOVA [52], while the validity of the model was confirmed with checking the lack-of-fit of the model. The ANOVA data (including sum of squares, mean square, F-value and Prob > F values, R^2, Adj-R^2, Pred-R^2, Adeq-R^2) for all the models are listed in Table 3. For each response (*i.e.*, $Rs_{(avg)}$ and t_R), the sum of squares of the model and residue error were calculated at first. Next, we obtain the mean square by dividing the sum of squares with the degree of freedom. In addition, the F-value, which is used to compare two sample variances, was calculated by dividing model mean square with residual mean square. Prob > F is the probability value that is associated with the F-value. In general, a term that has a Prob > F-value less than 0.05 would be considered a significant effect, while a Prob > F-value greater than 0.10 is generally regarded as not significant. Furthermore, the lack-of-fit values, which are part of the residues, are also reported to evaluate the validity of the model.

The data listed in Table 3 revealed that the models for responses ($Rs_{(avg)}$ and t_R) of the proteins are all significant (with a Prob > F-value less than 0.05). In addition, note that the lack-of-fit values are not significant (with a Prob > F-value greater than 0.1), which reveals that all the models fit well. For example, in case of $Rs_{(avg)}$ the "Lack-of-fit F-value" of 5.75×10^{-2} implies the Lack-of-fit is not significant relative to the pure error. There is a 5.23% chance that a "lack-of-fit F-value" this large could occur due to noise. Non-significant lack-of-fit means the model gives a good fit.

In order to further investigate the fitness of the models, the R^2 (multiple correlation coefficient), Adj-R^2, Pred-R^2 and adequate precision values (Adeq-R^2) for the models are evaluated as listed in Table 3. For a good statistical model, R^2 value should be close to 1.0 and difference between adj-R^2 and pred-R^2 should be within 0.2. For all the models, the three values are all in acceptable range.

Table 3
Analysis of variance (ANOVA) table used in the optimization of concentration of polymerization mixture.

Responses	Source	Sum of squares	Degree of freedom	Mean square	*F*-Value[a]	Prob > *F*[b]	R^2	Adj-R^2	Pred-R^2	Adeq-R^2
$Rs_{(avg)}$	Model	2.13×10^2	14	15.2	23.8	<0.0001				
	Residual (error)	5.75	9	6.39×10^{-1}						
	Lack-of-fit	2.30×10^{-1}	4	5.75×10^{-2}	5.23×10^{-2}	0.9930	0.97	0.93	0.85	18
	Pure error	5.52	5	1.10						
	Corrected total	2.19×10^2	23							
t_R	Model	1.72×10^3	14	1.22×10^2	20.6	<0.0001				
	Residual (error)	53.4	9	5.93						
	Lack-of-fit	18.4	4	4.60	6.56×10^{-1}	0.6483	0.97	0.92	0.75	18
	Pure error	35.0	5	7.01						
	Corrected total	1.77×10^3	23							

[a] The *F*-value for a term is the test for comparing the variance associated with that term with the residual variance. It is the mean square for the term divided by the mean square for the residual.
[b] This is the probability value that is associated with the *F*-value for this term. It is the probability of getting an *F*-value of this size if the term did not have an effect on the response. In general, a term that has a probability value less than 0.05 would be considered a significant effect. A probability value greater than 0.10 is generally regarded as not significant.

Table 3 also lists the Adeq-R^2. This value is an index of the signal to noise ratio and a value bigger than 4 suggests that the model gives a good fit. The Adeq-R^2 of the models are both 18 and this indicates that the models can be used to navigate the design space [53].

3.1.3. *Effects of the composition of polymerization mixture on the chromatographic properties*

Fig. 2(A and B) shows the regression coefficient plots for the two responses. The 95% confidence interval is expressed in terms of error bar over the coefficient. If the coefficient is smaller than the interval, it indicates that the coefficient is not significantly different from zero. As a result the corresponding factor is considered to be insignificant. The coefficients of the second-order terms will not be discussed in the following sections because of their lack of chemical denotations [54].

From the regression coefficient plots, it is obvious that the terms D (% (w/w) 1,4-butanediol) and E (% (w/w) water) have positive effect on the responses ($Rs_{(avg)}$ and t_R). One possible reason is that the increase of % (w/w) 1,4-butanediol and % (w/w) water will hasten the onset of the phase separation during the polymerization process resulting in the formation of relatively smaller cluster and smaller macropores [14]. Hence, a larger surface area is obtained resulting in higher resolution. In addition, according to the theory that the retention time is largely dependent on the size of the macropores [46]. Therefore, higher weight fraction of 1,4-butanediol and water will make a monolithic column with smaller macropore size, which influences the speed of the eluent flow and therefore the speed of the analysis.

A close examination of Fig. 2(A and B) revealed that besides the first-order terms, two cross terms (CE and DE) are significant to $Rs_{(avg)}$ and t_R. The significance of these cross terms indicates that although the single term is not significant, but when they combine with other terms they are significant. For example, term C (*i.e.*, % (w/w) 1-propanol), is not significant to $Rs_{(avg)}$ or t_R, however, it is significant as a cooperative term when combined with term E (*i.e.*, % (w/w) water).

Contour plots, based on the calculated models, provide direct information about the predicted responses because contour lines (also called isoresponse lines) with the same predicted values of the considered response provide valuable insights for the optimization of the factors. Fig. 3(A and B) shows the 2D contours plots for $Rs_{(avg)}$ and t_R, respectively. For each response, the three most significant factors were set as the *X*1-, *X*2- and *X*3-axes and the other two factors were fixed. In our case, % (w/w) AAUA, % (w/w) 1,4-butanediol and % (w/w) water are the three most significant factors for $Rs_{(avg)}$ and t_R, so these three factors at the corners indicated by B, E and C are set as the three *X*-axes, while the other two factors (% (w/w) EDMA and % (w/w) 1-propanol) were fixed. Each corner of the plots corresponds to the points representing the upper limit of each factor and the side opposite the corner represents the lower limit of the corresponding factor. For example, in Fig. 3A, the corner indicated with B stands for the upper limit defined for the % (w/w) AAUA, by moving away from this point, % (w/w) AAUA decrease. The constraints of the factors (shown in Table 1) define the plot region and this lead to some complex regions, which cannot be covered by the mixture design (*i.e.*, the grey-colored regions in the 2D contour plots). From the 2D contour plots (shown in Fig. 3(A and B)), it can be seen that, with the increase of %water, decrease of %1-propanol, and increase of %AAUA, higher resolution and longer retention time could be obtained.

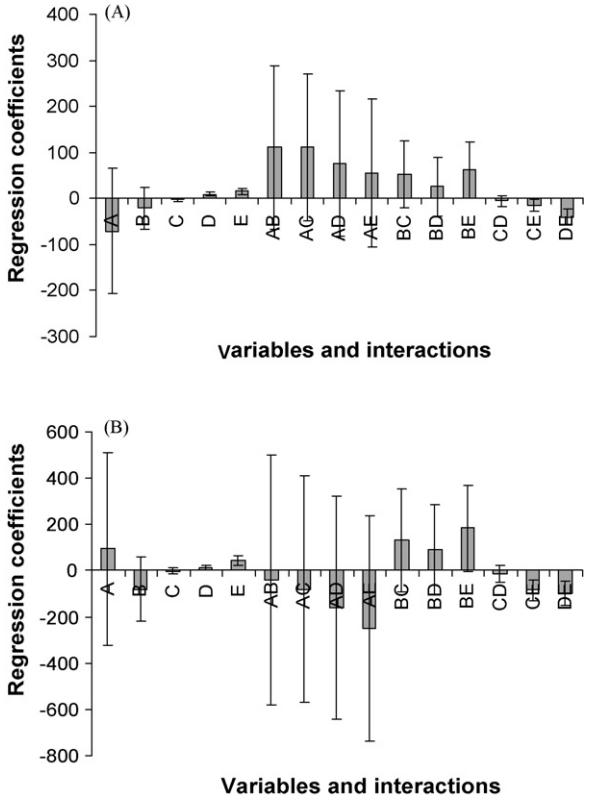

Fig. 2. The regression coefficients plots for proteins separation. (A) Average resolution ($Rs_{(avg)}$); (B) analysis time (t_R).

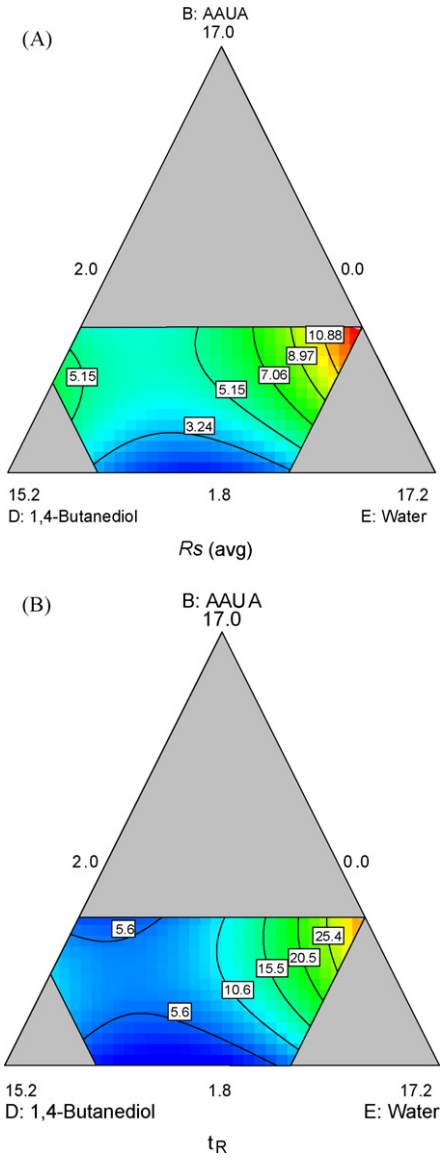

Fig. 3. The 2D contour plots obtained for (A) $Rs_{(avg)}$ and (B) t_R of proteins as a function of significant factors. %AAUA, %water and %1-propanol are the *X*1-, *X*2-, and *X*3-axes, respectively, with EDMA fixed at 18.5% and 1-propanol fixed at 62%.

3.2. Optimum polymerization mixture composition for separation of proteins

From the contour plots shown in Fig. 3(A and B), it appears that the polymerization conditions required to optimized $Rs_{(avg)}$ are in conflict with the values needed to optimize the t_R. One way to address this problem is to apply Derringer's desirability function $D(X)$. This function calculates the geometric mean of all transformed responses in the form of Eq. (4):

$$D = (d_1 \times d_2 \times \cdots \times d_n)^{1/n} = \left(\prod_{i=1}^{n} d_i\right)^{1/n} \quad (4)$$

where d_i is the response (in our case, $Rs_{(avg)}$ and t_R for the three proteins) to be optimized, n is the number (in our case, two) of the response in the mixture design. D is the desirability that ranges from 0 (the least desirable) to 1 (the most desirable). Using the Design-Expert software it was possible to obtain the best trade-off between $Rs_{(avg)}$ and t_R for proteins separation based on the given criteria.

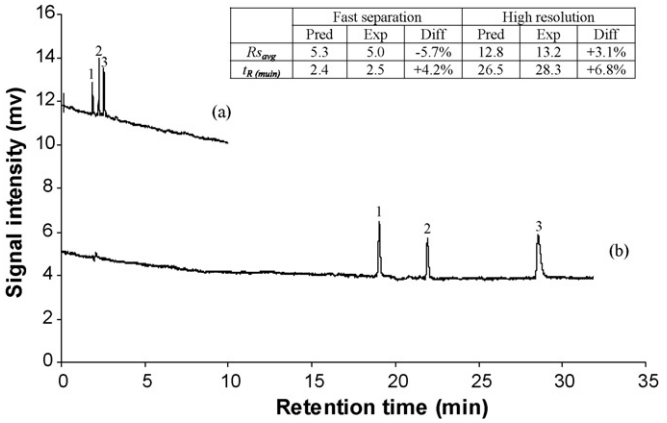

	Fast separation			High resolution		
	Pred	Exp	Diff	Pred	Exp	Diff
Rs_{avg}	5.3	5.0	-5.7%	12.8	13.2	+3.1%
$t_{R\,(min)}$	2.4	2.5	+4.2%	26.5	28.3	+6.8%

Fig. 4. Chromatograms of protein separations using (a) fast separation column OF-1 and (b) optimized high resolution column OH-1. Other conditions are the same as Fig. 1. The inset table describes the differences between predicted values and experimental values.

The characteristics of a goal may be altered by adjusting the importance of different responses. In the desirability objective function D(X), each response can be assigned an importance relative to the other responses. Importance (r_i) varies from the least important (a value of 1), to the most important (a value of 5). If varying degrees of importance are assigned to the different responses, the objective function is Eq. (5):

$$D = (d_1^{r_1} \times d_2^{r_2} \times \cdots \times d_n^{r_n})^{1/\sum r_i} = \left(\prod_{i=1}^{n} d_i^{r_i}\right)^{1/\sum r_i} \quad (5)$$

If all the responses are equally important, the simultaneous objective function reduces to the normal form of desirability.

Since the purpose of this study is to find the optimum polymerization mixtures for fast protein separation and high resolution protein separation, respectively, two different optimization criteria were set to achieve the goals. Hence, different importance values were set for the responses. If fast protein separation is desired, the best compromise between analysis time *versus* resolution was achieved by, setting a value of 5 for the minimization of t_R, while for $Rs_{(avg)}$, the assigned values were 1. The desired requests were fulfilled by the software using the solution (20.3% EDMA, 7.0% AAUA, 68.3% 1-propanol, 0% 1,4-butanediol and 3.9% water) with a *D* value of 0.84. For high resolution separation of protein, to obtain the best compromise between retention *versus* resolution, an importance value of 5 was assigned for the maximization of $Rs_{(avg)}$, while for t_R, importance value was 1. The software provided the desired requests by the solution (19.7% EDMA, 7.0% AAUA, 60.3% 1-propanol, 1.0% 1,4-butanediol and 11.5% water) with a *D* value of 0.81.

3.3. Chromatographic properties of the optimized columns

Chromatograms of the protein separation using the optimized monolithic columns are shown in Fig. 4. Judging from the chromatograms, three proteins could be separated in 2.5 min with an average resolution 5.0 on the optimum fast separation column (OF-1), while, the same analytes could be separated in 28.3 min with average resolution as high as 13.2 using the optimized high resolution column (OH-1).

In order to evaluate the feasibility of this experimental design approach, the differences between the predicted values (which come from the model) and the experimental values (which come from the real experimental) with the optimized column were compared. The results are listed as an inset table in Fig. 4. For the fast

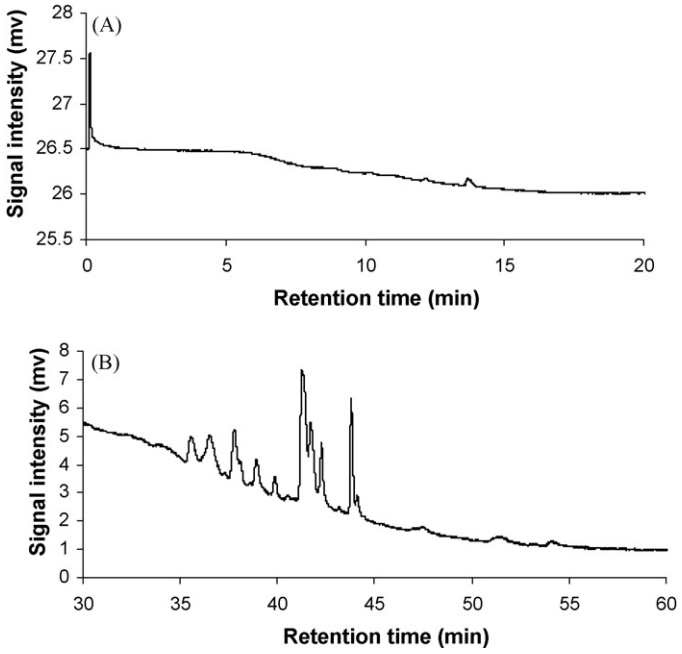

Fig. 5. Protein digest separation using the (A) optimized fast separation column OF-1 and (B) high resolution column OH-1. Conditions: mobile phase A: 98% ACN with 0.1% TFA in water; mobile phase B: 2% ACN with 0.1% TFA in water; linear gradient program, 16% A at 0 min, 20% A at 10 min, 50% A at 15 min, 80% A at 20 min; injection volume, 100 nL; flow rate, 1.1 μL/min; detection, 214 nm. Sample, 1.0 mg/mL myoglobin tryptic digest in water.

separation column, the experimental $Rs_{(avg)}$ and t_R are 5.7% and 4.2% different from the predicted values, respectively. For the high resolution column, the $Rs_{(avg)}$ and t_R are 3.1% and 6.8% different from the predicted values, respectively. All the differences between the experimental and predicted values are within the acceptable ranges, hence, this mixture experiment design and the optimization was proved to be valid and successful.

A tryptic digest of myoglobin was used to further evaluate the performance of the optimized high resolution column in μ-HPLC. Compared with the fast separation column OF-1 (Fig. 5(A)) where only few small peaks are seen, the high resolution column OH-1 (Fig. 5(B)), could successfully separate 14 peaks of the tryptic digest of myoglobin.

4. Properties of the monolithic columns

4.1. Morphology of the monolithic columns

Morphology of the monolith is one of the key factors affecting the separation capability of the polymeric monolithic column. To obtain high efficiency, homogeneity and rigidity of the polymer bed is needed [55]. Fig. 6 demonstrates the SEM pictures of 3 synthesized monolithic columns, which includes the column 7 (Fig. 6A), column 10 (Fig. 6B), the optimized fast separation column OF-1 (Fig. 6C) and optimized high resolution column OH-1 (Fig. 6D). It is clear that the morphology of the poly(AAUA-co-EDMA) monolith formed in columns 7 and OF-1 are very similar, but quite different from column OH-1. Furthermore, note that, column 7, which provides very fast elution (in 1.9 min), has the biggest clusters and largest through pores. The optimized fast separation monolith (column OF-1) consists of loosely connected microspheres and larger through pores. These structural features make possible the high permeability and convection mass transfer. On the other hand, column OH-1, the optimized high resolution column, contains tightly connected microspheres and smaller through pores resulting in higher surface area.

4.2. Porosity of the monolithic columns

First, the porosity of the monolith prepared in capillary was examined by a flow method [1], during which the monolith was solvated with mobile phase. In summary, the mobile phase linear velocity was measured by an inert dead volume tracer (thiourea) and the volumetric flow rate was also measured. Next, with the known empty tube dimensions, the total porosity ε_T was calculated (see Section 2). As shown in Table 4, the total porosities of the examined monoliths 7, 10, OF-1 and OH-1 were 91%, 72%, 79% and 73%, respectively, which seems to be consistent to the SEM micrographs shown in Fig. 6.

When the monolithic columns were prepared, parallel polymerization in glass vials under the same condition with the same mixtures were also conducted. Nitrogen adsorption and MIP_y experiments were performed to test the porosity of the monolith in dry state. The trend in the total porosity (ε_T and ε_T' shown in Table 4) tested by MIP_y correlates well with the flow method. However, the ε_T' values, determined using MIP_y, are a little lower than the values calculated by the flow method. These lower values obtained by the former method could be due to the differences in the state of sample (wet vs. dry). In addition, the polymerization container (the flow method sample was polymerized in capillary column while the MIP_y sample was polymerized in glass vials) may have also influenced the ε_T [42].

In addition to the determination of ε_T, several other physical parameters [cumulative pore volume (V) and bulk density (d)] of the monoliths can be determined from MIP_y method (Table 4). The V is generally represented as the void volume per unit mass (mm^3/g) of the solid material. The value of d is calculated from the ratio of total pore volume and the pore area. Using the BET method the surface area (r) was determined. The r of a solid material is its total surface area, which is in contact with the external environment. As expected, the poly(AAUA-co-EDMA) column 7 and column OF-1 showed similar d and r. For example, the pore diameter of these two monolithic columns is much larger and the surface area is much smaller compared to the monolithic columns 10 and OH-1, which provide the highest HPLC resolution and retention. Furthermore, the lowest V and ρ values obtained for column 1 agrees well with the lowest ε_T value obtained using both MIP_y method and the flow method.

Table 4
Pore characteristics of monolithic columns (columns 7, 10, OF-1 and OH-1): total porosity ε_T (determined with flow method), ε_T' permeability K^0, pore volume V, average pore diameter d, bulk density ρ (determined with MIP_y), and surface area r (determined with BET).

Column	Determined with flow method		Determined with MIP_y and BET				
	ε_T	K^0 (m^2)	V [mm^3/g]	d [μm]	ε_T'	ρ [g/m^3]	r [m^2/g]
7	91%	2.23×10^{-12}	2908	0.32	77%	0.26	6
10	72%	4.60×10^{-14}	1830	0.14	70%	0.38	25
OF-1	79%	1.33×10^{-12}	2840	0.30	72%	0.26	10
OH-1	73%	5.30×10^{-14}	1970	0.16	71%	0.36	27

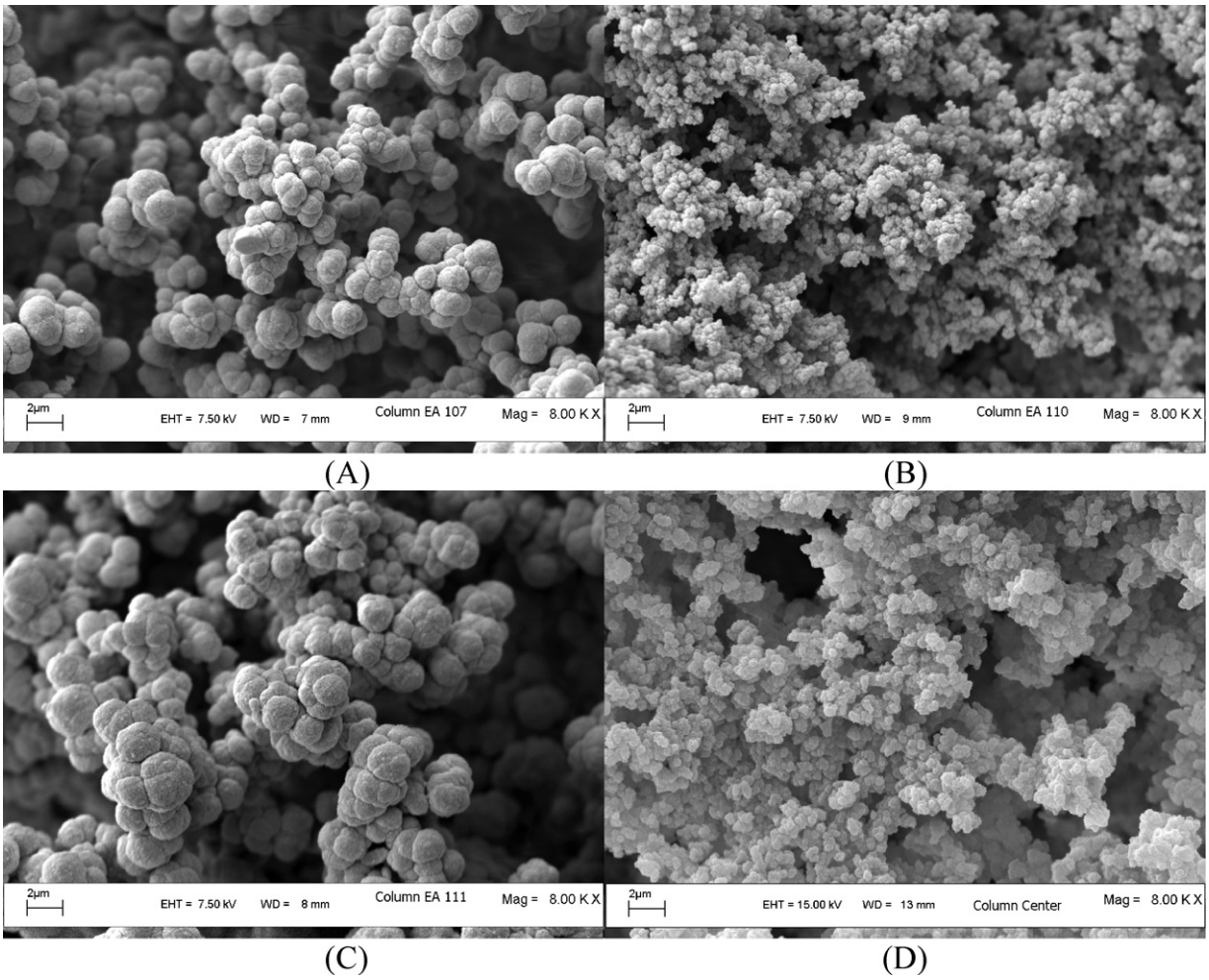

Fig. 6. Scanning electron micrographs of monolith columns. (A) Column 7; (B) column 10; (C) column OF-1. (D) Column OH-1. Detailed information of the polymerization mixture composition for the monolith is described in Table 2 and Section 3.2.

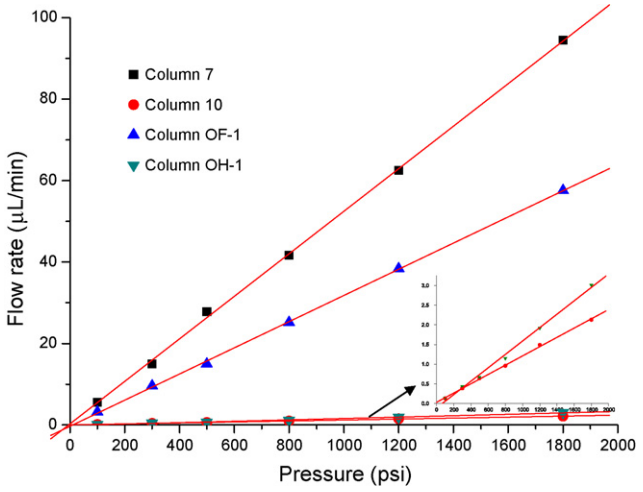

Fig. 7. Plots of the volumetric flow rate of mobile phase against the applied pressure. The composition of columns 7, 10, OF-1 and OH-1 are described in Table 2 and Section 3. Mobile phase, 60% ACN in water. All data were collected on μ-HPLC system. The inset plot shows the expanded trend obtained on column 10 and column OH-1.

4.3. Mechanical stability and permeability of the monolithic columns

Acetonitrile was used for the measurement of the pressure drop across the columns at different flow rates, which could also be used to indicate the mechanical stability and permeability of the columns [2]. For the three monolithic columns (7, 10, OF-1 and OH-1), the specific permeability K^0 was 2.23×10^{-12} m^2, 4.60×10^{-14} m^2, 1.33×10^{-12} m^2 and 5.30×10^{-14} m^2, respectively. The monolithic columns have a surprisingly high permeability value, which are at least two orders higher than that of the 3 μm particle-packed capillary column [56]. This is mainly due to the high total porosity of the monolith allowing liquids to flow through the column under low pressure. Plots of the volumetric flow rate of ACN against the applied pressure for the monolithic columns are shown in Fig. 7. For each column, the back pressure's dependency against flow rate of the solvent is a straight line with the correlation coefficient R better than 0.999. This indicated that permeability and mechanical stability of the monolith are both excellent.

4.4. Stability and reproducibility

Stability and reproducibility are two crucially important parameters for chromatographic columns. To evaluate the chromatographic stability, monolithic column made with the optimized polymerization mixture was utilized to conduct 5 injections on a daily basis for 3 consecutive days (*i.e.*, a total of 15 injections were

Table 5
Intra-day and inter-day reproducibility of retention time for proteins in μ-HPLC using columns OF-1 and OH-1 for consecutive 3 days. Other conditions are the same as Fig. 1.

Day no.	Run	Column OF-1 t_R (min) (%RSD)			Column OH-1 t_R (min) (%RSD)		
		Ri A	Cyo C	Myo	Ri A	Cyo C	Myo
1	5	2.03 (0.43)	2.35 (0.55)	2.62 (0.20)	18.57 (0.85)	21.69 (0.82)	28.32 (0.43)
2	5	2.02 (0.41)	2.34 (0.53)	2.63 (0.26)	19.07 (0.83)	22.07 (0.43)	28.13 (0.74)
3	5	2.03 (0.49)	2.36 (0.48)	2.63 (0.21)	18.74 (0.46)	21.87 (0.59)	27.92 (0.66)
Over all	15	2.03 (0.75)	2.35 (0.59)	2.63 (0.38)	18.79 (0.93)	21.88 (0.83)	28.12 (0.76)

Table 6
Intra-batch and inter-batch reproducibility of retention time of proteins in μ-HPLC using column OF-1 and OH-1. Other conditions are the same as Fig. 1.

Batch no.	Column	Column OF-1 t_R (min) (%RSD)			Column OH-1 t_R (min) (%RSD)		
		Ri A	Cyo C	Myo	Ri A	Cyo C	Myo
1	3	2.03 (1.50)	2.31 (1.09)	2.63 (0.88)	18.65 (1.61)	21.69 (1.13)	28.32 (1.11)
2	3	2.02 (0.56)	2.34 (1.01)	2.62 (1.05)	18.93 (1.47)	21.35 (1.95)	28.56 (1.41)
3	3	2.03 (1.23)	2.30 (0.91)	2.58 (1.03)	19.07 (1.34)	22.05 (1.58)	28.61 (1.22)
Overall	9	2.03 (1.76)	2.31 (1.09)	2.61 (1.15)	18.88 (2.11)	21.70 (2.33)	28.50 (1.59)

performed on this column). For the 2 optimized columns (OF-1 and OH-1), the relative standard deviation (RSD) values of the retention times and number of plates are shown in Table 5. For column OF-1, it was found that the inter-day precision of retention time ranged between 0.20% and 0.53%. The intra-day precision of retention time as the mean of 3 days ranged between 0.38% and 0.75%. For column OH-1, it was found that the inter-day precision of retention time ranged between 0.43% and 0.85%. The intra-day precision of retention time as the mean of 3 days ranged between 0.76% and 0.93%. Thus, the chromatographic performance stability of this new kind of monolith is acceptable.

To study the batch-to-batch column reproducibility, three batches of column were prepared and for each batch, 3 columns were made using the same polymerization mixture. Hence, a total of 9 columns were made in three batches to study the preparation reproducibility. From the results shown in Table 6, it was found that for column OF-1 all the RSD values of the retention time were lower than 1.76%, and for column OH-1 all the RSD values of the retention time were lower than 2.33%, which shows that the preparation of the monolith is reproducible.

5. Conclusions

A novel surfactant based poly(AAUA-co-EDMA) monolith was prepared as one-step polymerization (after the synthesis of AAUA monomer). The optimization of the polymerization mixture (concentration of crosslinker, monomer and progens) was achieved using a D-optimal mixture design. It was found that concentration of 1,4-butanediol and water are the two most important parameters in a successful monolith formation. Optimum polymerization mixture for fast separation column and high resolution column were processed by using a desirability function in the experimental design. The final optimized polymerization conditions predicted from the desirability function was tested. The experimental data were in very good to excellent agreement with the predicted results. The results showed that the D-optimal method is a very promising approach to obtain truly optimum polymerization conditions, allowing the successful development of new monolithic stationary phase. The physical and chromatographic properties of the optimized monolithic column were thoroughly investigated. The column presented typical polymer-based monolith morphology, excellent permeability and good mechanical stability. Furthermore, this kind of monolithic column demonstrated good inter- and intra-day repeatability as well as excellent the inter- and intra-batch reproducibility of column fabrication.

Acknowledgements

This work was supported by grant from the National Institutes of Health (Grant No. 2RO1-062314), The American Chemistry Society Petroleum Research Fund (47774-AC7) and Georgia State University Scholarly Support Grant.

References

[1] I. Gusev, X. Huang, C. Horvath, J. Chromatogr. A 855 (1999) 273.
[2] H. Oberacher, C.G. Huber, Trac-Trends Anal. Chem. 21 (2002) 166.
[3] I.L. Davies, K.D. Bartle, P.T. Williams, G.E. Andrews, Anal. Chem. 60 (1988) 204.
[4] W.R. LaCourse, C.O. Dasenbrock, Anal. Chem. 70 (1998) 37.
[5] Y. Song, Y.M. Liu, J. Mass Spectrom. 43 (2008) 1285.
[6] C.A. Hughey, B. Wilcox, C.S. Minardi, C.W. Takehara, M. Sundararaman, L.M. Were, J. Chromatogr. A 1192 (2008) 259.
[7] L. Tastet, D. Schaumloffel, B. Bouyssiere, R. Lobinski, Talanta 75 (2008) 1140.
[8] G. Guiochon, J. Chromatogr. A 1168 (2007) 101.
[9] F. Svec, C.G. Huber, Anal. Chem. 78 (2006) 2100.
[10] K. Stulik, V. Pacakova, J. Suchankova, P. Coufal, J. Chromatogr. B 841 (2006) 79.
[11] K. Won Ro, R. Nayak, D.R. Knapp, Electrophoresis 27 (2006) 3547.
[12] B. Gu, Z. Chen, C.D. Thulin, M.L. Lee, Anal. Chem. 78 (2006) 3509.
[13] M. Barut, A. Podgornik, P. Brne, A. Štrancar, J. Sep. Sci. 28 (2005) 1876.
[14] L. Rieux, H. Niederländer, E. Verpoorte, R. Bischoff, J. Sep. Sci. 28 (2005) 1628.
[15] Q. Zhao, X.-F. Li, X.C. Le, Anal. Chem. 80 (2008) 3915.
[16] A. Juan-Garcia, G. Font, Y. Pico, J. Chromatogr. A 1153 (2007) 104.
[17] C. Yu, F. Svec, J.M.J. Frechet, Electrophoresis 21 (2000) 120.
[18] A. Pena, D. Chmielova, C.M. Lino, P. Solich, J. Sep. Sci. 30 (2007) 2924.
[19] A. Detroyer, S. Stokbroekx, H. Bohets, W. Lorreyne, P. Timmerman, P. Verboven, D.L. Massart, Y. VanderHeyden, Anal. Chem. 76 (2004) 7304.
[20] A. Detroyer, Y. VanderHeyden, K. Reynaert, D.L. Massart, Anal. Chem. 76 (2004) 1903.
[21] G. Gübitz, M.G. Schmid, Biopharm. Drug Dispos. 22 (2001) 291.
[22] D. Šatínskí, P. Chocholouš, M. Salabová, P. Solich, J. Sep. Sci. 29 (2006) 2494.
[23] S. Eeltink, F. Svec, Electrophoresis 28 (2007) 137.
[24] C. Viklund, F. Svec, J.M.J. Frechet, K. Irgum, Chem. Mater. 8 (1996) 744.
[25] M. Lammerhofer, F. Svec, J.M.J. Frechet, W. Lindner, J. Chromatogr. A 925 (2001) 265.
[26] R. Fraile, V. Sánchez, J. High Resolut. Chromatogr. 16 (1993) 169.
[27] A.B. Baranda, N. Etxebarria, R.M. Jimenez, R.M. Alonso, Talanta 67 (2005) 933.
[28] L.V. Candioti, J.C. Robles, V.E. Mantovani, H.C. Goicoechea, Talanta 69 (2006) 140.
[29] L.-H. Chang, T.-T. Jong, H.-S. Huang, Y.-F. Nien, C.-M.J. Chang, Sep. Purif. Technol. 47 (2006) 119.
[30] N.M. de Aragao, M.C.C. Veloso, M.S. Bispo, S.L.C. Ferreira, J.B. de Andrade, Talanta 67 (2005) 1007.
[31] D. De Faveri, P. Torre, P. Perego, A. Converti, J. Food Eng. 61 (2004) 407.
[32] Y. Li, H.D. Tolley, M.L. Lee, Anal. Chem. 81 (2009) 4406.
[33] I. Nischang, F. Svec, J.M.J. Frechet, J. Chromatogr. A 1216 (2009) 2355.
[34] L. Trojer, S.H. Lubbad, C.P. Bisjak, G.K. Bonn, J. Chromatogr. A 1117 (2006) 56.
[35] J.G. Hou, S.A.A. Rizvi, J. Zheng, S.A. Shamsi, Electrophoresis 27 (2006) 1263.
[36] R. Iqbal, S.A.A. Rizvi, S.A. Shamsi, Electrophoresis 26 (2005) 4127.
[37] S.A. Shamsi, R. Iqbal, C. Akbay, Electrophoresis 26 (2005) 4138.
[38] C. Akbay, S.A.A. Rizvi, S.A. Shamsi, Anal. Chem. 77 (2005) 1672.
[39] S.A.A. Rizvi, S.A. Shamsi, Electrophoresis 26 (2005) 4172.

[40] K.W. Yeoh, C.H. Chew, L.M. Can, L.L. Koh, H.H. Teo, J. Macromol. Sci., Pure Appl. Chem. A 26 (1989) 663.
[41] C. Gu, L. Lin, X. Chen, J. Jia, J. Ren, N. Fang, J. Sep. Sci. 30 (2007) 1005.
[42] C. Gu, L. Lin, X. Chen, J. Jia, J. Ren, N. Fang, J. Chromatogr. A 1170 (2007) 15.
[43] E.C. Peters, M. Petro, F. Svec, J.M.J. Frechet, Anal. Chem. 70 (1998) 2288.
[44] A.R. Ivanov, C. Horváth, B.L. Karger, Electrophoresis 24 (2003) 3663.
[45] V.M. Meyers, Practical High-Performance Liquid Chromatography, Wiley, New Jersey, 2005.
[46] I. Tanret, D. Mangelings, Y. VanderHeyden, J. Pharmaceut. Biomed. 48 (2008) 264.
[47] W. Bragg, D. Norton, S.A. Shamsi, J. Chromatogr. B 875 (2008) 304.
[48] M.J. Anderson, P.J. Whitcomb, Mixture DOE uncover formulations quicker (Technical note), Rubber and Plastic news, October 21, 2002, http://www.rubbernews.com.
[49] M.P. Barrioulet, N. Delaunay-Bertoncini, C. Demesmay, J.L. Rocca, Electrophoresis 26 (2005) 4104.
[50] J. Grafnetter, P. Coufal, E. Tesarova, J. Suchankova, Z. Bosakova, J. Sevcik, J. Chromatogr. A 1049 (2004) 43.
[51] E.F.H. Sebastiaan Eeltink, L. Geiser, F. Svec, J.M.J. Fréchet, G.P. Rozing, P.J. Schoenmakers, W.Th. Kok, J. Sep. Sci. 30 (2007) 407.
[52] S. Furlanetto, S. Orlandini, A.M. Marras, P. Mura, S. Pinzauti, Electrophoresis 27 (2006) 805.
[53] B. Chauhan, R. Gupta, Process Biochem. 39 (2004) 2115.
[54] J. He, S.A. Shamsi, J. Chromatogr. A 1216 (2009) 845.
[55] L. Cong, B. Huang, Q. Chen, B. Lu, J. Zhang, Y. Ren, Anal. Chim. Acta 569 (2006) 157.
[56] C.K. Ratnayake, C.S. Oh, M.P. Henry, J. Chromatogr. A 887 (2000) 277.